The recurrent *de novo* c.2011C>T missense variant in *MTSS2* causes syndromic intellectual disability

Authors

Yan Huang, Gabrielle Lemire, Lauren C. Briere, ..., David A. Sweetser, Kym M. Boycott, Hugo J. Bellen

Correspondence

hbellen@bcm.edu

A cohort of five unrelated individuals with the same heterozygous *de novo* variant in MTSS2 (GenBank: NM_138383.2: c.2011C>T [p.Arg671Trp]), present with syndromic mild intellectual disability. Modeling in *Drosophila* suggested that the variant had decreased normal function and increased toxicity compared to the reference MTSS2 and may act as a dominant-negative allele.

Huang et al., 2022, The American Journal of Human Genetics *109*, 1923–1931
October 6, 2022

https://doi.org/10.1016/j.ajhg.2022.08.011

The recurrent *de novo* c.2011C>T missense variant in *MTSS2* causes syndromic intellectual disability

Yan Huang,[1,2,12] Gabrielle Lemire,[3,4,12] Lauren C. Briere,[5,6,12] Fang Liu,[7] Marja W. Wessels,[8] Xueqi Wang,[3] Matthew Osmond,[3] Oguz Kanca,[1,2] Shenzhao Lu,[1,2] Frances A. High,[5] Melissa A. Walker,[9] Lance H. Rodan,[10] Undiagnosed Diseases Network, Care4Rare Canada Consortium, Michael F. Wangler,[1,2] Shinya Yamamoto,[1,2] Kristin D. Kernohan,[3,11] David A. Sweetser,[5,6] Kym M. Boycott,[3] and Hugo J. Bellen[1,2,*]

Summary

MTSS2, also known as MTSS1L, binds to plasma membranes and modulates their bending. *MTSS2* is highly expressed in the central nervous system (CNS) and appears to be involved in activity-dependent synaptic plasticity. Variants in *MTSS2* have not yet been associated with a human phenotype in OMIM. Here we report five individuals with the same heterozygous *de novo* variant in *MTSS2* (GenBank: NM_138383.2: c.2011C>T [p.Arg671Trp]) identified by exome sequencing. The individuals present with global developmental delay, mild intellectual disability, ophthalmological anomalies, microcephaly or relative microcephaly, and shared mild facial dysmorphisms. Immunoblots of fibroblasts from two affected individuals revealed that the variant does not significantly alter MTSS2 levels. We modeled the variant in *Drosophila* and showed that the fly ortholog *missing-in-metastasis* (*mim*) was widely expressed in most neurons and a subset of glia of the CNS. Loss of *mim* led to a reduction in lifespan, impaired locomotor behavior, and reduced synaptic transmission in adult flies. Expression of the human *MTSS2* reference cDNA rescued the *mim* loss-of-function (LoF) phenotypes, whereas the c.2011C>T variant had decreased rescue ability compared to the reference, suggesting it is a partial LoF allele. However, elevated expression of the variant, but not the reference *MTSS2* cDNA, led to similar defects as observed by *mim* LoF, suggesting that the variant is toxic and may act as a dominant-negative allele when expressed in flies. In summary, our findings support that *mim* is important for appropriate neural function, and that the *MTSS2* c.2011C>T variant causes a syndromic form of intellectual disability.

MTSS2 (MIM: 616951), also known as MTSS1L (MTSS I-BAR domain containing 2), is a member of a family consisting of five proteins sharing a conserved I-BAR (inverse BAR) domain at the N terminus, as well as an actin-binding WH2 (WASP-homology 2) domain at the C terminus.[1–3] I-BAR domains generate inverse membrane curvature and induce formation of plasma membrane protrusions when expressed in cells by binding to the inner leaflet of membranes through their convex lipid-binding interface.[4,5] Based on structural features and phylogenetic relationships, MTSS2 and its paralog MTSS1 belong to the Mim (missing-in-metastasis) subfamily.[1,6] In addition to the I-BAR and WH2 domains, MTSS2 also contains a serine-rich region, three proline-rich motifs, and a leucine zipper motif (Figure 1A).[2] Human *MTSS2* is mainly expressed in the CNS while *MTSS1* is expressed at variable levels in most tissues (GTex).[7] Mouse *Mtss2* has been shown to be highly expressed in fetal radial glia, which are multipotent cells involved in neuronal migration, neurogenesis, and gliogenesis in the developing CNS.[2] In adult mice, *Mtss2* is predominantly expressed in the cerebellum but not the hippocampus; however, hippocampal expression can be highly induced by synaptic activity such as exercise and may promote dendritic spine formation of neurons.[2,8] Variants in *MTSS2* have not been previously linked to any genetic disorder in OMIM.

Through genomic matchmaking, including the use of the MatchMaker Exchange[9] and one-sided matchmaking strategies,[10] we identified a cohort of five individuals affected by an intellectual disability syndrome who all carry the same *de novo* heterozygous (GenBank: NM_138383.2: c.2011C>T [p.Arg671Trp]) variant in *MTSS2* (Table 1). Informed consent was obtained from the five families. The five individuals range in age from 18 months to 42 years. Individual 2 is the only adult. The five individuals present with mild developmental delay and/or intellectual disability. Individuals 1 and 2 have a developmental coordination disorder. Individuals 1 and 3 have been diagnosed with autism spectrum disorder. Individual 2 developed adult-onset focal absence seizures, which are well controlled with one

[1]Department of Molecular and Human Genetics, Baylor College of Medicine (BCM), Houston, TX 77030, USA; [2]Jan and Dan Duncan Neurological Research Institute, Texas Children's Hospital, Baylor College of Medicine, Houston, TX 77030, USA; [3]Children's Hospital of Eastern Ontario Research Institute, University of Ottawa, Ottawa, ON K1H 8L1, Canada; [4]Broad Center for Mendelian Genomics, Program in Medical and Population Genetics, Broad Institute of MIT and Harvard, Cambridge, MA 02142, USA; [5]Division of Medical Genetics & Metabolism, Massachusetts General Hospital for Children, Boston, MA 02114, USA; [6]Center for Genomic Medicine, Massachusetts General Hospital, Boston, MA 02114, USA; [7]Department of Pediatrics, Bethune International Peace Hospital, Shijiazhuang 050082, Hebei, China; [8]Department of Clinical Genetics, Erasmus Medical Center, University Medical Center Rotterdam, Rotterdam, the Netherlands; [9]Department of Neurology, Division of Neurogenetics, Child Neurology, Massachusetts General Hospital, Boston, MA 02114, USA; [10]Department of Neurology, Boston Children's Hospital, Boston, MA 02115, USA; [11]Newborn Screening Ontario, Children's Hospital of Eastern Ontario, Ottawa, ON K1H 8L1, Canada
[12]These authors contributed equally
*Correspondence: hbellen@bcm.edu
https://doi.org/10.1016/j.ajhg.2022.08.011.

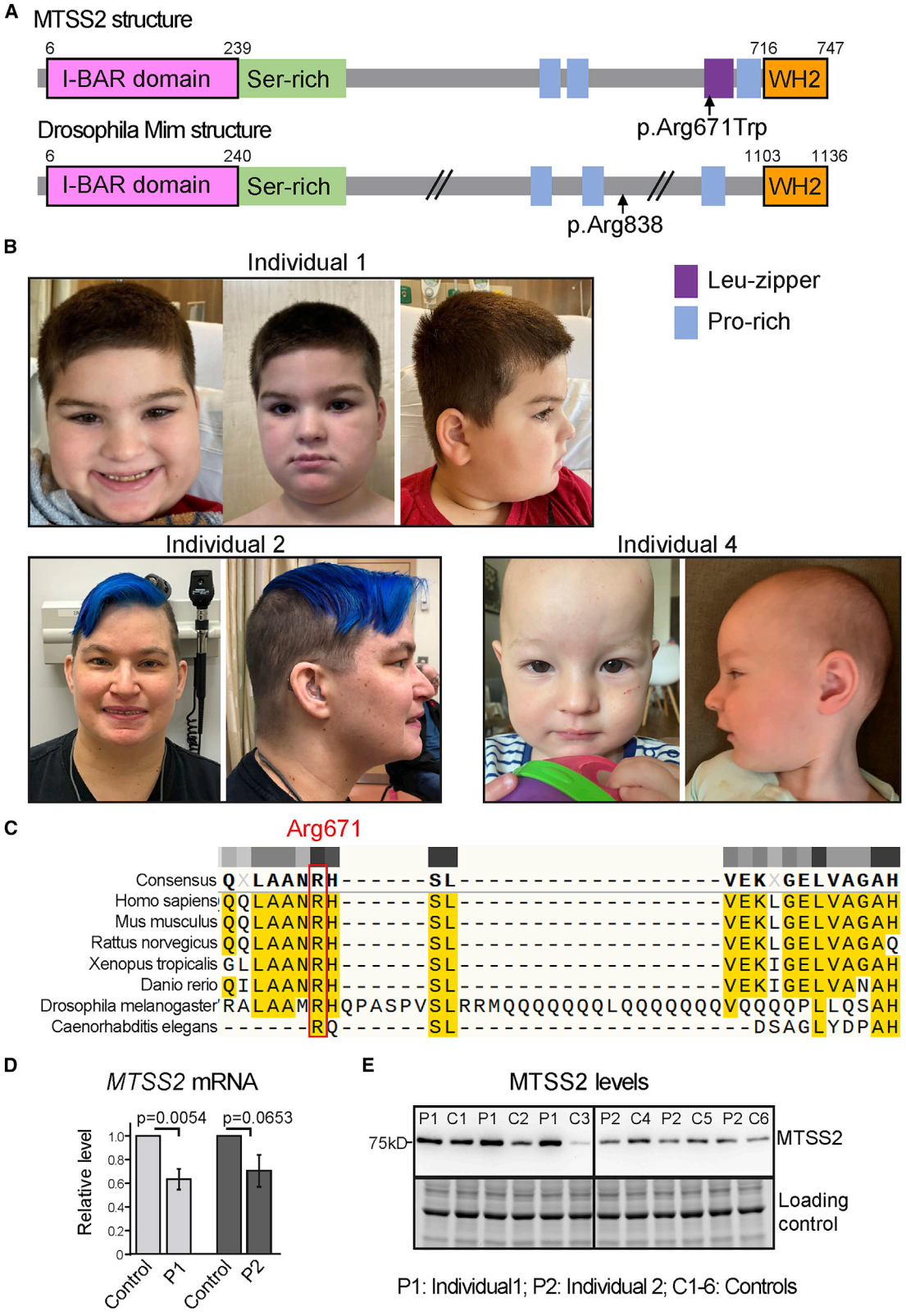

Figure 1. Genetic and clinical information of the c.2011C>T variant in *MTSS2*

(A) Structure of the MTSS2 protein (GenBank: NM_138383.2; NP_612392.1) and the position of the c.2011C>T (p.Arg671Trp) variant. MTSS2 is composed of an N-terminal I-BAR domain, a serine-rich region, three proline-rich motifs, a leucine zipper motif, and a C-terminal WH2 domain (upper panel). The structure of *Drosophila* Mim protein (GenBank: NM_001259228; NP_001246157.1) with indication of the corresponding Arg (p.Arg838). The breaks represent stretches of unaligned sequences (lower panel).

(B) Three affected individuals share the following facial dysmorphisms: long upslanting palpebral fissures, bitemporal narrowing, arched eyebrows, thickened ear helices, and epicanthal folds. Individual 1 at 8 years old; individual 2 at 42 years old; individual 4 at 15 months of age.

(legend continued on next page)

Table 1. Main clinical features of five unrelated individuals with a *de novo* c.2011C>T (p.Arg671Trp) variant in *MTSS2* (GenBank: NM_138383.2)

Individual	1	2	3	4	5
Age[a]	8 yo	42 yo	15 yo	14 months	21 months
Sex	male	female	male	male	male
Ethnicity	European	European	European	European	Chinese
ID or GDD[b]	mild ID	mild ID	mild ID	GDD	GDD
Autism spectrum disorder	+	–	+	N/A[b]	N/A[b]
Seizures	–	+	–	–	–
Ophthalmological anomalies	nystagmus, foveal hypoplasia	optic atrophy	nystagmus, ptosis	bilateral iris cysts	nystagmus, ptosis
Sensorineural hearing loss	+	+	U[b]	–	–
Distinctive facial features[c]	+	+	+	+	U[b]
Microcephaly or relative microcephaly (head circumference centile)[d]	+ (40%)	+ (<0.1%, −2.9 SD)	+ (2%)	+ (2%)	+ (<0.1%, −2.6 SD)
Height centile[d]	83%	60%	U[b]	91%	70%

[a]Age at last clinical evaluation.
[b]Abbreviations: ID, intellectual disability; GDD, global developmental delay (individuals 4 and 5 are too young to be evaluated for ID); N/A, not applicable; U, unknown.
[c]Upslanting palpebral fissures, epicanthal folds, bitemporal narrowing.
[d]Centiles based on WHO growth curves and Nellhaus head circumference curves.[11,12]

antiepileptic drug (topiramate). The remaining four individuals have not had any reported seizures, and individual 1 has had normal electroencephalograms. Individuals 2 and 5 have microcephaly, whereas the other three individuals have a relative microcephaly with head circumferences that are low compared to their heights (Table 1). A review of facial photographs from individuals 1, 2, 3, and 4 reveals shared mild dysmorphic features including long upslanting palpebral fissures, bitemporal narrowing, arched eyebrows, and epicanthal folds (Figure 1B).

While all but individual 2 have normal vision, all five individuals present with ophthalmological anomalies (Table 1). Three individuals have nystagmus and two have ptosis, but the other ocular anomalies are not present in more than one individual in this cohort. Individual 1 has a mild form of congenital foveal hypoplasia, and individual 4 has bilateral iris cysts. Individual 2, the only adult, has a history of progressive bilateral optic atrophy, first noted at age 13, and is now legally blind.

Individual 2 developed progressive bilateral sensorineural hearing loss requiring bilateral hearing aids that started in late childhood, and her hearing loss has now been stable for more than 10 years. Individual 1 passed hearing screens at birth and at 19 months of age but was found to have mild bilateral sensorineural hearing loss at 8 years of age. The hearing status of individual 3 is unknown, and individuals 4 and 5 are reported to have normal hearing, but they did not undergo a hearing test.

From the available records, there does not appear to be any clearly consistent brain magnetic resonance imaging (MRI) findings across this cohort. Of the four individuals who have had brain MRIs, two were reported as normal (individuals 3 and 4), two showed dissymmetry of the corpus callosum, dysmorphic hippocampi, and mildly dysmorphic lateral ventricles (individuals 1 and 2; Figure S4), one showed possible mild cerebellar atrophy (individual 1; Figure S4A), and one showed delayed myelination of cerebral white matter and mildly dysmorphic lateral ventricles (individual 5). No anomalies of the white matter or cerebral or cerebellar atrophy were seen on the brain MRI of individual 2 in adulthood. Additional clinical information for all five individuals can be found in Table S1.

Trio exome sequencing for the five individuals identified a *de novo* heterozygous variant in *MTSS2* (GenBank: NM_138383.2: c.2011C>T [p.Arg671Trp]). To gather information about the gene in human and model organisms,

(C) The human MTSS2 p.Arg671 (GenBank: NP_612392.1) is present in all species listed: mouse (GenBank: NP_941027.1), rat (GenBank: NP_001178487.1), *Xenopus* (GenBank: XP_031756693.1), zebrafish (GenBank: XP_005170001.1), *Drosophila* (GenBank: NP_001246157.1), and *C. elegans* (GenBank: NP_001317862.1).
(D) Real-time PCR shows decreased MTSS2 expression compared to age-matched control subjects in fibroblasts from individuals 1 and 2. Error bars: SEM. p values were calculated by unpaired t test.
(E) Immunoblot of MTSS2 in fibroblasts from individual 1 and individual 2 show no consistent changes of protein levels across affected individuals and control subjects. Total protein served as a loading control. P1, individual 1; P2, individual 2; C1–C6, age- and sex-matched control subjects from 6 individuals.

we queried the Model organism Aggregated Resources or Rare Variant ExpLoration (MARRVEL).[13] The loss-of-function (LoF) observed/expected (o/e) score for *MTSS2* is 0.15, and the probability of being LoF intolerant (pLI) score is 0.98, suggesting that *MTSS2* is intolerant to LoF alleles.[14] The c.2011C>T variant is absent from gnomAD,[14] and is located at an evolutionarily conserved residue (Figures 1C and S1A). Multiple *in silico* prediction programs (see supplemental methods) predict that this missense change has a deleterious effect on MTSS2, including a CADD score[15] of 25. No other variants in known or novel genes have been retained as plausible candidates by exome analysis for the five individuals. In summary, we suspected that the *de novo* c.2011C>T variant explains the individuals' phenotypes given the deleterious *in silico* predictions, absence of this variant in population databases, the involvement of *MTSS2* in neuron physiology, and the identification of an overlapping phenotype in five unrelated individuals with the same *de novo* missense variant. The mechanism by which the c.2011C>T variant affects the function of MTSS2 could be haploinsufficiency, gain-of-function (hypermorph or neomorph) or a dominant-negative action (antimorph), although the recurrent nature of the variant increases the likelihood of the latter two mechanisms.[16]

We evaluated the impact of c.2011C>T by assessing mRNA and protein levels from individual 1- and 2-derived fibroblasts compared to age- and sex-matched control subjects. Real-time PCR analysis showed a reduction of *MTSS2* transcript level ($p = 0.0054$ in individual 1 and $p = 0.0653$ in individual 2; Figure 1D). However, western blot analysis showed variable levels of MTSS2, and the affected individuals' levels appeared within the normal range (Figure 1E). These data suggest that the variant leads to a decrease in mRNA level, but this may not affect the level of MTSS2 in fibroblasts.

To investigate the function of the *MTSS2* variant, we modeled the variant in *Drosophila melanogaster*. Drosophila *mim* (*missing-in-metastasis*) is the ortholog of human *MTSS2* and *MTSS1* with DIOPT scores[17] of 6/16 and 7/16, respectively. Although the fly Mim contains unaligned sequence stretches and is larger than the human MTSS2 (Figure 1A) as well as MTSS1, Mim and MTSS2 share 46% similarity and 31% identity of the protein sequences. The leucine zipper motif is disrupted by the unaligned stretches, but the overall protein structures are similar, and the major domains of MTSS2 and MTSS1 are present in the fly protein (Figures 1A and S1B).[18] Furthermore, the residue affected by the c.2011C>T (p.Arg671Trp) variant in MTSS2 is conserved in fly Mim (Figure 1C).

First we generated a $mim^{T2A\text{-}GAL4}$ allele by inserting a *CRISPR-Mediated Integration Cassette* (*CRIMIC*) in a shared intron of all *mim* transcripts.[19] The splice acceptor (SA) allows the *T2A-GAL4* to be incorporated into the mRNA and the poly(A) tail leads to transcription termination and truncates the *mim* mRNA (Figure 2A). In addition, the viral *T2A* sequence arrests translation but allows the production of GAL4,[20] which is under the control of endogenous regulatory elements of *mim*.[21,22] Therefore, the $mim^{T2A\text{-}GAL4}$ allele is able to drive expression of any *UAS-cDNA* in the same pattern as *mim*.[23] Our real-time PCR data indicate that the transcript levels of two exons which are adjacent to the interrupted intron are not detected in $mim^{T2A\text{-}GAL4}/mim^{T2A\text{-}GAL4}$ larvae (Figure 2B), indicating that the *T2A-GAL4* truncates the *mim* transcript and is therefore likely a severe LoF allele.

Given the neurological deficits in all the identified individuals and given that *MTSS2* is highly expressed in the mammalian CNS (GTEx),[2,7] we explored the expression of *mim* in the fly CNS. We used the $mim^{T2A\text{-}GAL4}$ to drive expression of *UAS-mCD8-RFP* to label the membranes of the cells that express *mim* and found a widespread expression of *RFP* in the third instar larval and adult brain (Figures 2C and 2I). This included the mushroom body (insect neurons that play a critical role in learning and memory), the optic lobe, and the ventral nerve cord (the spinal cord equivalent in insects). We used the *UAS-NLS-mCherry* to label the nuclei of the cells that expressed *mim* (Figures 2D and 2J). By comparing its expression to the pan-neuronal nuclear marker Elav and the nuclear glial marker Repo, the nature of the cells expressing *mim* could be easily identified. In the larval CNS, *mCherry* (*mim*) was expressed primarily in neurons (Figures 2E and 2F) and in some glia in the ventral nerve cord (Figures 2G and 2H). In the adult brain, *mCherry* (*mim*) was expressed in most neurons as well as many glia of the central brain and optic lobe (Figures 2K–2N). This was consistent with single-cell RNA-seq data from the Fly Cell Atlas (Figure S2).[24,25] Of note, *mim* was highly expressed in neurons of the mushroom body (Figures 2C–2E and 2I). In summary, *mim* was widely expressed in neurons as well as in some glia of developing larval CNS and adult brain, and expression was particularly enriched in the neurons that mediate learning and memory.

The $mim^{T2A\text{-}GAL4}$ efficiently truncates the *mim* transcript (Figure 2B), and flies that carry $mim^{T2A\text{-}GAL4}$ over a chromosomal deficiency allele *Df(2R)Exel6051* that lacks *mim* (~120 kb; *Df* for short) all survived to adulthood, suggesting that the gene is not essential for development and viability. However, flies that are homozygous $mim^{T2A\text{-}GAL4}/mim^{T2A\text{-}GAL4}$ showed a low eclosion rate, as only 10% of the expected number of flies develop into adults at 25°C (Figure 3A). This suggests that the $mim^{T2A\text{-}GAL4}$ contains an off-target second mutation(s) that reduces the viability of homozygous *mim* mutants. To assess the function of human *MTSS2*, we generated transgenic flies that carry *UAS-MTSS2* cDNAs. The eclosion rate of $mim^{T2A\text{-}GAL4}/mim^{T2A\text{-}GAL4}$ mutants was partially but significantly rescued by expression of the human *UAS-MTSS2* reference cDNA (from 10% to 50%). This partial rescue suggests that the absence of *mim* enhances lethality of the off-target mutation(s) and hence reduces the eclosion rate to 10% when homozygous. However, this rescue was not observed by expression of the c.2011C>T variant (Figures 3A and S3A), suggesting that it is a LoF variant.

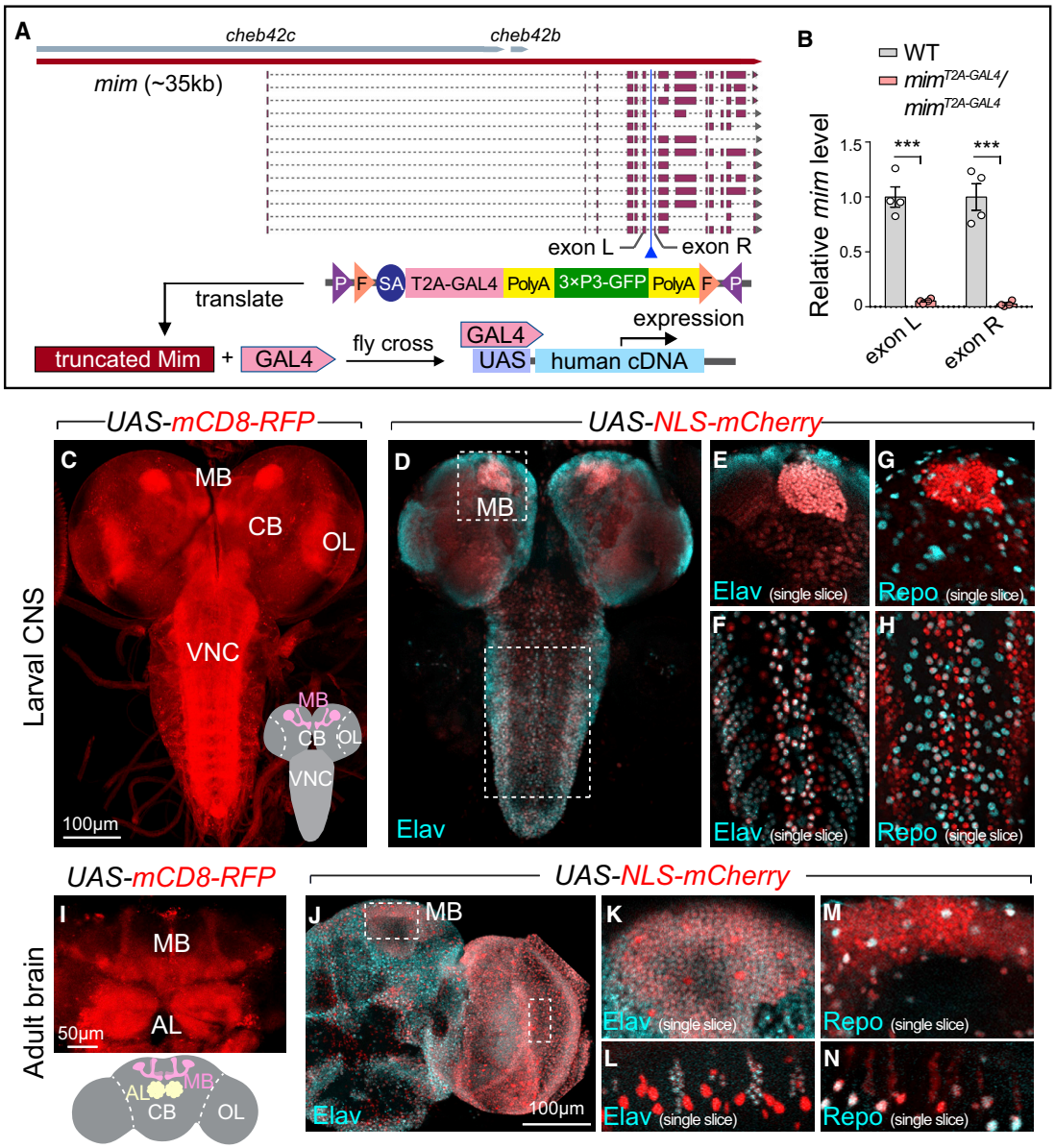

Figure 2. ***mim*$^{T2A\text{-}GAL4}$ is expressed in many neurons and some glia**

(A) Structure of fly *mim* and *T2A-GAL4* allele. *cheb42b* and *cheb42c* are nested genes in the *mim* locus. The *CRIMIC T2A-GAL4* sequence is inserted into a shared intron of all *mim* transcripts, truncating the transcript and protein while expressing T2A-GAL4.[20,23] P, attP; F, FRT; SA, splice acceptor.

(B) *mim* mRNA expression based on real-time PCR of exon L (left) and R (right) that adjacent to the inserted intron is not detected in homozygous *mim*$^{T2A\text{-}GAL4}$ mutant larvae when compared to wild-types (*w1118*). Exon L and R are shared exons of all transcripts that are indicated in (A). mRNA levels were normalized to that of housekeeping gene *rpl32*. Error bar: SEM. ***$p < 0.001$ by unpaired t tests.

(C) Whole-mount, projection image of larval central nervous system (CNS) from *mim*$^{T2A\text{-}GAL4}$/+; *UAS-mCD8-RFP*/+ (cell membrane) showing *mim* is highly expressed in mushroom body (MB) in the central brain (CB), optic lobe (OL), and ventral nerve cord (VNC). Schematic of larval CNS shows the different structures.

(D) Projection image of larval CNS co-stained with neuronal marker anti-Elav from *mim*$^{T2A\text{-}GAL4}$/+; *UAS-NLS-mCherry*/+ (cell nuclei).

(E–H) Single-focal images of mushroom body (MB) (E and G) and ventral nerve cord (VNC) (F and H) co-stained with anti-Elav (E and F) and anti-Repo (G and H).

(I) Projection image of adult central brain (CB) from *mim*$^{T2A\text{-}GAL4}$/+; *UAS-mCD8-RFP*/+ showing *mim* is highly expressed in mushroom body (MB) and antennal lobe (AL). Below: schematic of adult brain.

(J) Projection image of half of an adult brain from *mim*$^{T2A\text{-}GAL4}$/+; *UAS-NLS-mCherry*/+ co-stained with anti-Elav.

(K–N) Single-slice confocal images of adult mushroom body (MB) and optic lobe (OL) co-stained with anti-Elav (K and L) and anti-Repo (M and N).

Although *mim*$^{T2A\text{-}GAL4}$/*Df* mutants showed no obvious defects in eclosion rate, their lifespan was significantly shorter than control flies that are heterozygous *mim*$^{T2A\text{-}GAL4}$/+ and carry an empty control UAS (*robo1*$^{T2A\text{-}GAL4}$/+; *UAS-empty*/+) at 29°C. Expression of *UAS-MTSS2* reference in the *mim*$^{T2A\text{-}GAL4}$/*Df* mutants fully rescued the lifespan,

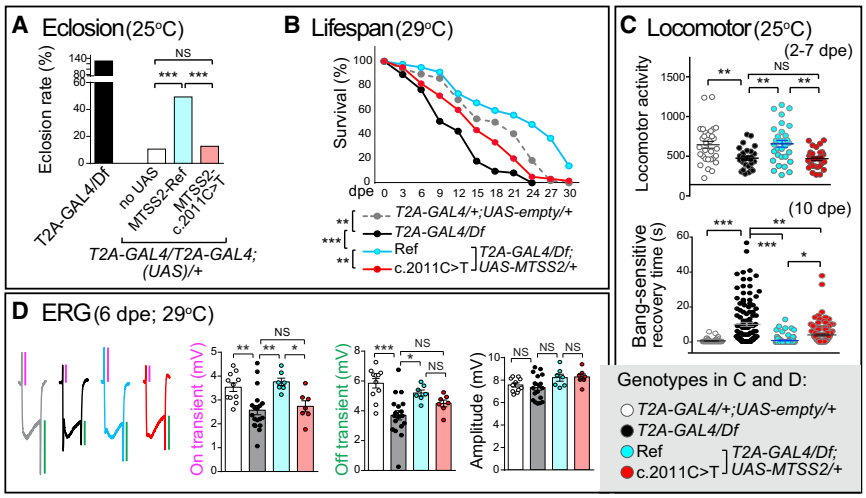

Figure 3. Expression of human *MTSS2* reference rescues the defects in *mim* LoF flies, whereas c.2011C>T variant showed decreased rescue ability

(A) Eclosion rates of adult flies of the indicated genotypes. Numbers of analyzed flies are in Figure S3A. NS, $p > 0.05$; ***$p < 0.001$ based on chi-squared tests between each genotype.

(B) Lifespan of adult flies with indicated genotypes. $n > 60$ flies for each genotype; **$p < 0.01$, ***$p < 0.001$ by chi-squared test for trend between each genotype.

(C) Locomotor activity of flies at 2–7 days post eclosion (dpe) of indicated genotypes measured by DAM assay, $n = 32$ flies for each genotype (top). Recovery time (s) after bang-sensitivity induced by 15 s vortex of flies at 8 dpe, $n > 50$ flies for each genotype (bottom). Error bar: SEM. *$p < 0.05$, **$p < 0.01$, ***$p < 0.001$ based on one-way ANOVA with Tukey's multiple comparison test between each indicated genotype.

(D) Electroretinograms (ERGs) of flies at 6 dpe. On (indicated as magenta), Off (indicated as green) transients and amplitudes were quantified. Error bar: SEM. NS, $p > 0.05$; *$p < 0.05$, **$p < 0.01$, ***$p < 0.001$ by one-way ANOVA with Tukey's multiple comparison test between each indicated genotype.

whereas the c.2011C>T variant only partially rescued the reduced lifespan (Figure 3B).

The expression level of human *MTSS2* is highest in the cerebellum and spinal cord (GTEx).[7] Fly *mim* is also highly expressed in the ventral nerve cord (Figure 2C), which corresponds to the vertebrate spinal cord. To determine whether *mim* plays a role in locomotor behavior of flies, we first performed Drosophila Activity Monitoring (DAM) assay[26] of adult flies at 25°C. $mim^{T2A\text{-}GAL4}/Df$ mutants showed a significant decrease in locomotor activity when compared to control flies ($mim^{T2A\text{-}GAL4}/+$; *UAS-empty/+*). This decrease in activity was fully rescued by expression of *UAS-MTSS2* reference allele but not the c.2011C>T variant (Figures 3C and S3B). Next, we did bang-sensitivity testing, which is an assay to assess neuronal dysfunction. Upon vortexing the flies for 10–15 s, wild-type flies recover in less than a few seconds and do not exhibit seizures. However, some flies with genotypes that are susceptible to seizures become paralyzed, uncoordinated, or shake, exhibiting a seizure-like phenotype, and these flies can take a significantly longer time to recover than wild-type flies.[27–29] The $mim^{T2A\text{-}GAL4}/Df$ mutants showed bang-sensitivity and recovered slowly to an upright position after vortexing for 15 s. Expression of *UAS-MTSS2* reference partially rescued the bang-sensitivity phenotype and significantly shortened the recovery time; however, c.2011C>T expression had decreased rescue ability (Figure 3C).

Ophthalmological defects appeared to be a common clinical finding in the cohort of affected individuals with the c.2011C>T variant, with one individual having significant progressive optic atrophy. The fly *mim* is highly expressed in the optic lobe (Figures 2C and 2I) as well as in adult photoreceptors and lamina neurons in the eyes (Figure S2). To examine whether *mim* is required for visual function, we performed electroretinograms (ERGs) in adult flies. The amplitudes of the ERG traces represent the ability of photoreceptors to sense photons upon light exposure, while the On/Off transients provide a measure of synaptic transmission between photoreceptors and the postsynaptic neurons in the lamina.[30] The $mim^{T2A\text{-}GAL4}/Df$ mutants had significantly reduced On/Off transients, but the amplitude at 29°C was not affected (Figure 3D). This suggests that loss of *mim* does not affect phototransduction but that defects at the synapses between photoreceptors and postsynaptic neurons may be at play. Expression of *UAS-MTSS2* reference in $mim^{T2A\text{-}GAL4}/Df$ mutants fully rescued the On-transient decrease and partially rescued the Off-transient decrease, while the c.2011C>T variant showed very limited rescue for both transients (Figure 3D). In summary, *mim* LoF impairs lifespan, reduces locomotor activity, affects the bang sensitivity response, and impairs synaptic transmission in the visual system of adult flies. These defects were partially or fully rescued by expression of the human reference MTSS2, implicating functional conservation of human MTSS2 with the fly Mim. The c.2011C>T variant has significantly decreased rescue ability in all assays tested when compared to the reference allele, suggesting that it is a partial LoF allele.

The previous assays were focused on rescuing the severe LoF alleles with a reference or mutant cDNA copy. However, given that the variant of interest is a *de novo* recurrent dominant change, we investigated whether overexpression of the reference and the variant cDNAs induced different or similar phenotypes. This was done by driving the reference and variant *MTSS2* cDNAs in $mim^{T2A\text{-}GAL4}$ heterozygous flies. Expression of *UAS-MTSS2* reference in $mim^{T2A\text{-}GAL4}/+$ flies did not significantly affect lifespan or locomotor activity when compared to the $mim^{T2A\text{-}GAL4}/+$; *UAS-empty/+* controls. However, expression of the c.2011C>T variant caused

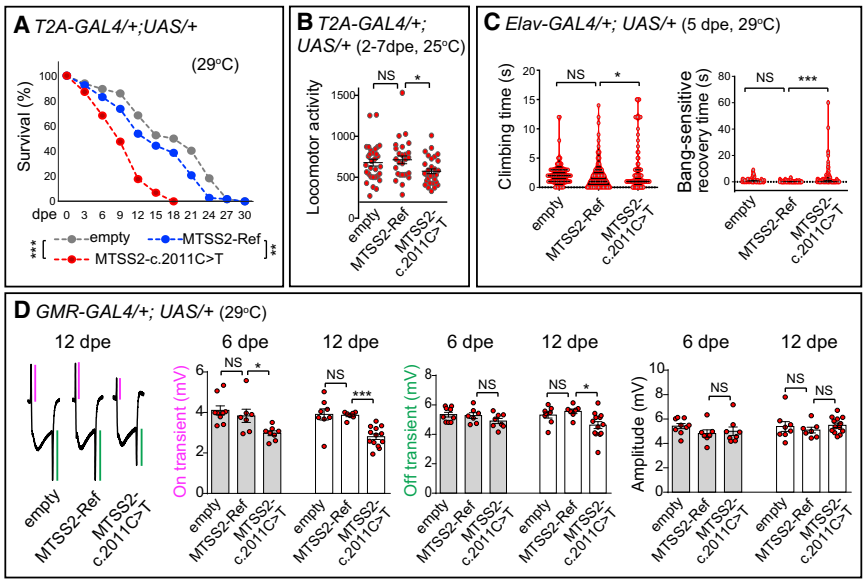

Figure 4. *MTSS2* c.2011C>T variant is toxic when expressed in flies

(A) Lifespan of adult flies with indicated genotypes. n > 100 flies for each genotype; **p < 0.01, ***p < 0.001 by chi-squared test for trend between each genotype.

(B) Locomotor activity of flies with indicated genotypes. Error bar: SEM. n = 32 flies for each genotype; *p < 0.05 by one-way ANOVA with Tukey's multiple comparison test between each indicated genotype.

(C) Climbing and bang-sensitivity assays of flies at 5 dpe, *UAS-cDNAs* were driven by *Elav-GAL4*. Error bar: SEM. n > 70 flies for each genotype; *p < 0.05, ***p < 0.001 by one-way ANOVA with Tukey's multiple comparison test between each indicated genotype.

(D) ERGs of flies expressing *UAS-cDNAs* under the control of *GMR-GAL4*. On and Off transients and amplitudes were quantified. Error bar: SEM. NS, p > 0.05; *p < 0.05, **p < 0.01 ***p < 0.001 by one-way ANOVA with Tukey's multiple comparison test between each indicated genotype.

defects in both assays (Figures 4A, 4B, and S3B), suggesting that expression of the variant is toxic. To further assess the toxicity associated with the c.2011C>T variant, we ectopically expressed it with tissue-specific GAL4s. Pan-neuronal (*Elav-GAL4*) expression of *UAS-MTSS2* c.2011C>T, but not the reference, led to mild but significant climbing defects and bang-sensitivity (Figure 4C). Moreover, expression of *UAS-MTSS2* c.2011C>T, but not the reference, in the eye using the *GMR-GAL4* caused a decrease in On/Off transients but again did not significantly affect the phototransduction pathway (Figure 4D). These data strongly suggest that the c.2011C>T acts as a dominant-negative or antimorphic allele. Interestingly, the ERG phenotype in flies at 12 days post eclosion (dpe) is slightly more severe than that at 6 dpe (Figure 4D), suggesting that the phenotypes associated with the c.2011C>T variant may become progressively worse with time.

In summary, exome sequencing combined with one-sided and two-sided matchmaking strategies resulted in the identification of five unrelated individuals with the same *de novo* c.2011C>T variant in *MTSS2* and an overlapping phenotype consisting of global developmental delay, mild intellectual disability, ophthalmological anomalies, microcephaly or relative microcephaly, and shared facial features. Two of the five individuals also have hearing loss. An age-related penetrance could explain why some of the clinical features that were of teen or adult onset in the oldest individual in this cohort—severe optic atrophy and seizures—are not present in younger individuals from this cohort (Table 1). The recurrent nature of the specific heterozygous c.2011C>T variant raised the possibility of a gain-of-function or dominant-negative mechanism. The fact that the MTSS2 level in fibroblasts from individuals 1 and 2 was not significantly altered compared to control subjects (Figure 1E) suggests that the variant protein was present in the affected individuals. Our fly studies revealed that *mim* is expressed in the ventral nerve cord, optic lobe, and eyes (Figures 2C and S2), and that its loss underlies defects in locomotor and visual functions (Figure 3). Importantly, the defects in *mim* LoF mutants were rescued by human *MTSS2*, implicating functional conservation between the two orthologs. The *MTSS2* c.2011C>T variant behaved as a partial LoF allele in a *mim* LoF background. Overexpression of the c.2011C>T variant caused similar phenotypes as the LoF, including shortened lifespan, decreased locomotor activity, bang-sensitivity, and abnormal communication between pre and postsynaptic cells (Figures 3 and 4). These data indicate that the MTSS2 c.2011C>T variant may interfere with the normal function of fly Mim by means of a dominant-negative effect.

The later onset of some neurological findings—optic atrophy and seizures—in the adult individual in this cohort suggests that this condition may have a slowly progressive clinical course, in line with our finding in flies that expression of the c.2011C>T variant leads to a progressively worsening ERG phenotype with age (Figure 4D). The expression of *MTSS2* mRNA in the mouse hippocampus is highly dynamic and activity dependent,[8] suggesting that neuronal activity may lead to the production of the reference protein as well as the toxic protein. The expression of *MTSS2* and *MTSS1* in the adult retina is not high (GTex),[7] suggesting that the retina does not require as high levels of MTSS proteins as the CNS, and one copy of the reference protein may be sufficient for its function. However, the retina could be sensitive to the presence of the toxic *MTSS2* allele; we hypothesize that the toxic protein is induced by synaptic activity in the optic nerves, becoming detrimental with age and causing progressive optic atrophy.

In conclusion, our findings demonstrate that the c.2011C>T variant in *MTSS2* causes an autosomal-dominant intellectual disability syndrome through a suspected dominant-negative mechanism. The identification and detailed phenotyping of additional affected individuals across their lifespan will be required to better define the natural history of this condition. If this neurodevelopmental disorder is confirmed to have a progressive nature, this creates an opportunity for potential therapeutic intervention to prevent the neurological deficits with a later age of onset.

Data and code availability

The variant in *MTSS2* was submitted to ClinVar (https://www.ncbi.nlm.nih.gov/clinvar/) (GenBank: NM_138383.2; accession numbers SCV001432151.1). The exome datasets supporting this study have not been deposited in a public repository because of ethical restriction.

Supplemental information

Supplemental information can be found online at https://doi.org/10.1016/j.ajhg.2022.08.011.

Acknowledgment

We thank all of the individuals and their families for their participation, in particular the parents of individual 4, who connected with the UDN directly about this gene. We thank Dr. Xiao Mao for connecting us with the clinician in China. We thank Hongling Pan for the injections to create transgenic flies. Part of this work was performed under the Care4Rare Canada Consortium. G.L. was supported by a Children's Hospital Academic Medical Organization clinical fellowship award through CHEO and by the Broad Institute of MIT and Harvard Center for Mendelian Genomics (grants UM1 HG008900, U01 HG0011755 and R01 HG009141). K.M.B. was supported by a CIHR Foundation Grant (FDN-154279) and a Tier 1 Canada Research Chair in Rare Disease Precision Health. This work was supported by the NIH Common Fund, through the Office of Strategic Coordination/Office of the NIH Direction under award number U01HG007690 (D.A.S., M.A.W., F.A.H., L.C.B., E.T.). The Translational Clinical Research Center at Massachusetts General Hospital was supported by NIH grant number 1UL1TR001102. H.J.B. was supported through the Model Organisms Screening Center of the UDN by U54NS093793 (NINDS), the Office of Research Infrastructure Programs of the NIH (awards R24 OD022005 and R24 OD031447). The content of this paper is solely the responsibility of the authors and does not necessarily represent official views of the NIH. Further acknowledgments are described in the supplemental information.

Declaration of interests

The authors declare no competing interests.

Received: June 1, 2022
Accepted: August 12, 2022
Published: September 5, 2022; corrected online October 21, 2022

Web resources

CADD, https://cadd.gs.washington.edu/
DIOPT, http://www.flyrnai.org/diopt
Fly Cell Atlas: Adult brain, https://scope.aertslab.org/#/FlyCellAtlas/FlyCellAtlas%2Fs_fca_biohub_head_10x.loom/gene
GeneMatcher, https://genematcher.org/
gnomAD, https://gnomad.broadinstitute.org/
GTEx, https://gtexportal.org/
L3 brain, http://scope.aertslab.org/#/Larval_Brain/*/welcome
MARRVEL, http://marrvel.org/
Matchmaker Exchange, https://www.matchmakerexchange.org/
Mutation Taster, http://www.mutationtaster.org/
OMIM, https://omim.org
PhenomeCentral, https://www.phenomecentral.org/
PolyPhen2, http://genetics.bwh.harvard.edu/pph2/
ShinyR-DAM, https://karolcichewicz.shinyapps.io/shinyr-dam
SIFT, https://sift.bii.a-star.edu.sg/

References

1. Yamagishi, A., Masuda, M., Ohki, T., Onishi, H., and Mochizuki, N. (2004). A novel actin bundling/filopodium-forming domain conserved in insulin receptor tyrosine kinase substrate p53 and missing in metastasis protein. J. Biol. Chem. *279*, 14929–14936.
2. Saarikangas, J., Hakanen, J., Mattila, P.K., Grumet, M., Salminen, M., and Lappalainen, P. (2008). ABBA regulates plasma-membrane and actin dynamics to promote radial glia extension. J. Cell Sci. *121*, 1444–1454.
3. Frost, A., Unger, V.M., and De Camilli, P. (2009). The BAR domain superfamily: membrane-molding macromolecules. Cell *137*, 191–196.
4. Saarikangas, J., Zhao, H., Pykäläinen, A., Laurinmäki, P., Mattila, P.K., Kinnunen, P.K.J., Butcher, S.J., and Lappalainen, P. (2009). Molecular mechanisms of membrane deformation by I-BAR domain proteins. Curr. Biol. *19*, 95–107.
5. Mattila, P.K., Salminen, M., Yamashiro, T., and Lappalainen, P. (2003). Mouse MIM, a tissue-specific regulator of cytoskeletal dynamics, interacts with ATP-actin monomers through its C-terminal WH2 domain. J. Biol. Chem. *278*, 8452–8459.
6. Pykäläinen, A., Boczkowska, M., Zhao, H., Saarikangas, J., Rebowski, G., Jansen, M., Hakanen, J., Koskela, E.V., Peränen, J., Vihinen, H., et al. (2011). Pinkbar is an epithelial-specific BAR domain protein that generates planar membrane structures. Nat. Struct. Mol. Biol. *18*, 902–907.
7. Consortium, G.T. (2013). The Genotype-Tissue Expression (GTEx) project. Nat. Genet. *45*, 580–585.
8. Chatzi, C., Zhang, Y., Hendricks, W.D., Chen, Y., Schnell, E., Goodman, R.H., and Westbrook, G.L. (2019). Exercise-induced enhancement of synaptic function triggered by the inverse BAR protein. Elife *8*, e45920.
9. Philippakis, A.A., Azzariti, D.R., Beltran, S., Brookes, A.J., Brownstein, C.A., Brudno, M., Brunner, H.G., Buske, O.J., Carey, K., Doll, C., et al. (2015). The Matchmaker Exchange: a platform for rare disease gene discovery. Hum. Mutat. *36*, 915–921.

10. Boycott, K.M., Azzariti, D.R., Hamosh, A., and Rehm, H.L. (2022). Seven years since the launch of the Matchmaker Exchange: The evolution of genomic matchmaking. Hum. Mutat. *43*, 659–667.
11. WHO Multicentre Growth Reference Study Group (2006). WHO Child Growth Standards based on length/height, weight and age. Acta Paediatr. Suppl. *450*, 76–85.
12. Nellhaus, G. (1968). Head circumference from birth to eighteen years. Practical composite international and interracial graphs. Pediatrics *41*, 106–114.
13. Wang, J., Al-Ouran, R., Hu, Y., Kim, S.Y., Wan, Y.W., Wangler, M.F., Yamamoto, S., Chao, H.T., Comjean, A., Mohr, S.E., et al. (2017). MARRVEL: Integration of Human and Model Organism Genetic Resources to Facilitate Functional Annotation of the Human Genome. Am. J. Hum. Genet. *100*, 843–853.
14. Karczewski, K.J., Francioli, L.C., Tiao, G., Cummings, B.B., Alföldi, J., Wang, Q., Collins, R.L., Laricchia, K.M., Ganna, A., Birnbaum, D.P., et al. (2020). The mutational constraint spectrum quantified from variation in 141, 456 humans. Nature *581*, 434–443.
15. Kircher, M., Witten, D.M., Jain, P., O'Roak, B.J., Cooper, G.M., and Shendure, J. (2014). A general framework for estimating the relative pathogenicity of human genetic variants. Nat. Genet. *46*, 310–315.
16. Muller, H.J. (1932). Further studies on the nature and causes of gene mutations. Int Congr Genet *6*.
17. Hu, Y., Flockhart, I., Vinayagam, A., Bergwitz, C., Berger, B., Perrimon, N., and Mohr, S.E. (2011). An integrative approach to ortholog prediction for disease-focused and other functional studies. BMC Bioinf. *12*, 357.
18. Quinones, G.A., Jin, J., and Oro, A.E. (2010). I-BAR protein antagonism of endocytosis mediates directional sensing during guided cell migration. J. Cell Biol. *189*, 353–367.
19. Kanca, O., Zirin, J., Garcia-Marques, J., Knight, S.M., Yang-Zhou, D., Amador, G., Chung, H., Zuo, Z., Ma, L., He, Y., et al. (2019). An efficient CRISPR-based strategy to insert small and large fragments of DNA using short homology arms. Elife *8*, e51539.
20. Diao, F., and White, B.H. (2012). A novel approach for directing transgene expression in Drosophila: T2A-Gal4 in-frame fusion. Genetics *190*, 1139–1144.
21. Lee, P.T., Zirin, J., Kanca, O., Lin, W.W., Schulze, K.L., Li-Kroeger, D., Tao, R., Devereaux, C., Hu, Y., Chung, V., et al. (2018). A gene-specific T2A-GAL4 library for Drosophila. Elife *7*, e35574.
22. Nagarkar-Jaiswal, S., Lee, P.T., Campbell, M.E., Chen, K., Anguiano-Zarate, S., Cantu Gutierrez, M., Busby, T., Lin, W.W., He, Y., Schulze, K.L., et al. (2015). A library of MiMICs allows tagging of genes and reversible, spatial and temporal knockdown of proteins in Drosophila. Elife *4*, e05338.
23. Kanca, O., Zirin, J., Hu, Y., Tepe, B., Dutta, D., Lin, W.W., Ma, L., Ge, M., Zuo, Z., Liu, L.P., et al. (2022). An expanded toolkit for Drosophila gene tagging using synthesized homology donor constructs for CRISPR mediated homologous recombination. Elife *11*, e76077.
24. Li, H., Janssens, J., De Waegeneer, M., Kolluru, S.S., Davie, K., Gardeux, V., Saelens, W., David, F.P.A., Brbić, M., Spanier, K., et al. (2022). Fly Cell Atlas: A single-nucleus transcriptomic atlas of the adult fruit fly. Science *375*, eabk2432.
25. Ravenscroft, T.A., Janssens, J., Lee, P.T., Tepe, B., Marcogliese, P.C., Makhzami, S., Holmes, T.C., Aerts, S., and Bellen, H.J. (2020). Drosophila Voltage-Gated Sodium Channels Are Only Expressed in Active Neurons and Are Localized to Distal Axonal Initial Segment-like Domains. J. Neurosci. *40*, 7999–8024.
26. Pfeiffenberger, C., Lear, B.C., Keegan, K.P., and Allada, R. (2010). Locomotor activity level monitoring using the Drosophila Activity Monitoring (DAM) System. Cold Spring Harb. Protoc. *2010*. pdb.prot5518.
27. Ganetzky, B., and Wu, C.F. (1982). Indirect Suppression Involving Behavioral Mutants with Altered Nerve Excitability in DROSOPHILA MELANOGASTER. Genetics *100*, 597–614.
28. Benzer, S. (1971). From the gene to behavior. JAMA *218*, 1015–1022.
29. Parker, L., Howlett, I.C., Rusan, Z.M., and Tanouye, M.A. (2011). Seizure and epilepsy: studies of seizure disorders in Drosophila. Int. Rev. Neurobiol. *99*, 1–21.
30. Dolph, P., Nair, A., and Raghu, P. (2011). Electroretinogram recordings of Drosophila. Cold Spring Harb. Protoc.. pdb.prot5549.